THE JOURNAL OF PHYSICAL CHEMISTRY C

Article

pubs.acs.org/JPCC

1,4-Benzenedimethanethiol Interaction with Au(110), Ag(111), Cu(100), and Cu(111) Surfaces: Self-Assembly and Dissociation Processes

Juanjuan Jia,[†,‡] Angelo Giglia,[§] Marcos Flores,[∥] Oscar Grizzi,[⊥] Luca Pasquali,[§,#,○] and Vladimir A. Esaulov*[,†,‡]

[†]Université-Paris Sud, Institut des Sciences Moléculaires d'Orsay, Orsay, Bâtiment 351, Université Paris Sud, 91405 Orsay, France

[‡]CNRS, UMR 8214, Institut des Sciences Moléculaires d'Orsay, Orsay, Bâtiment 351, Université Paris Sud, 91405 Orsay, France

[§]CNR-IOM, s.s.14, km 163.5 in Area Science Park, 34012 Trieste, Italy

[∥]Departamento de Fisica, Universidad de Chile, Av. Blanco Encalada 2008, Santiago, Chile

[⊥]Centro Atómico Bariloche-CNEA, Instituto Balseiro-UNC, CONICET, 8400 S.C. de Bariloche, Río Negro, Argentina

[#]Dipartimento di Ingegneria 'E. Ferrari', Università di Modena e Reggio Emilia, Via Vignolese 905, 41125 Modena, Italy

[○]Department of Physics, University of Johannesburg, P.O. Box 524, Auckland Park, 2006, South Africa

Supporting Information

ABSTRACT: In this work, we study systematically the evaporative adsorption under high vacuum conditions of 1,4-benzenedimethanethiol (BDMT) onto different metal surfaces: Ag(111), Au(110), Cu(100), and Cu(111). The study is carried out by photoemission using synchrotron radiation. In the case of Ag(111) and Au(110), at low exposures, a lying down BDMT phase is formed, with both S atoms attached to Ag and Au. A standing up phase is attained after a large exposure, above several hundred thousand Langmuir. However, also a mixed complex over layer appears to be formed, attributable to molecules sticking on top of the SAM. In the case of Au(110), heating leads to BDMT desorption with some degree of S−C bond scission, and some S atoms are left in different adsorption sites with mainly two different core level binding energies. On Ag(111), after heating the sample, BDMT desorbs and also sulfidation of Ag occurs. In the case of Cu(100) and Cu(111), S−C bond cleavage occurs already after initial adsorption. Lost S from BDMT molecules is adsorbed on Cu. Surface passivation occurs and only then BDMT adsorption takes place, with an interface with Cu enriched with sulfur.

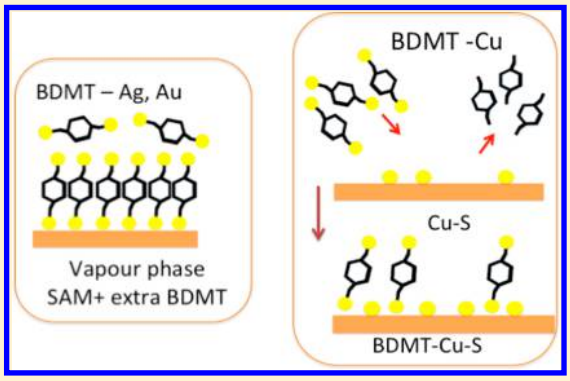

1. INTRODUCTION

In this paper, we examine the characteristics of dithiol films evaporated onto some coinage metals. Our interest in this subject is related to the possibility of bonding of the sulfur end terminals to metal electrode surfaces and thus formation of molecular bridges between two metallic entities. This possibility has attracted much attention in the context of developing sensors and applications in molecular electronics or in building various metal organic heterostructures.[1−10] A key requisite in these applications is that a free thiol termination be available to allow anchoring to the metallic entities. A number of works have therefore been devoted to dithiol self-assembly.[9−31] One of the main problems is that the dithiol could form a lying down phase with both ends bound to the surface, which then may be a hindrance for transition to a standing up phase.[19] It has also been found that there are solvent related effects[18,25,26,28] and photooxidation[12,13] problems rendering formation of high quality ordered self-assembled monolayers (SAMs) difficult. Thus, much debate exists around this problem.[14,19] However, it has been shown that formation of an initial lying down phase should in principle not stop the formation of a film[22,23] with standing up molecules. It was also shown that a judicious choice of the solvents and preparation procedure can indeed yield such ordered SAMs[9−11,18,24−27] on gold. An example is the case of 1,4-benzenedimethanethiol (BDMT) on Au(111), for which reflection adsorption infrared spectroscopy (RAIRS), spectroscopic ellipsometry, X-ray photoelectron spectroscopy (XPS),[24] NEXAFS,[27] and X-ray reflectivity[31] indicate that a standing up, ordered SAM is formed.

With few exceptions,[7,8] the dithiol SAMs have been prepared by immersion into a solution containing the dithiol. If however more reactive substrates are used, then evaporation in a vacuum could be more appropriate, since then clean dithiol−surface

Received: September 11, 2014
Revised: October 20, 2014
Published: October 20, 2014

interfaces could be formed and also modification of the thiol termination due to, e.g., photooxidation[12,13] would be avoided. Several experiments using the vapor phase adsorption have been performed,[7,8] including studies by some of us.[22,29,30] A study of BDMT evaporative adsorption on Au(111), performed by ion scattering,[30] indicated that a high fraction of the molecules are in a standing up configuration and the SAM is indeed S terminated. Interaction of thiols with more reactive substrates such as Ag and Cu has been investigated by several groups.[32−46] In a number of cases, well-ordered SAMs were found to be formed. For dithiols, it has been suggested that this may be less obvious,[45] but for BDMT, time-of-flight direct recoil spectroscopy (TOF DRS[47]) ion scattering measurements also indicate formation of a standing up SAM.[48,49] These measurements revealed some differences with respect to Au, and in particular for Cu, BDMT uptake was much faster; i.e., lower exposures were necessary. For the Cu(100) surface, a curious observation was the appearance of sulfur at very low exposures,[49] which was attributed to either segregation from the bulk or initial S−C bond scission. The latter has been reported in some other cases of thiol interaction with copper[33,34,38−40] though not for benzenethiol.[41]

The ion scattering results for Au,[30] Ag, and Cu[48,49] seem promising, but they did not give any information on the characteristics of the molecular film such as ordering, orientation, and the molecule−metal interface. This characterization is an essential prerequisite for the generalized and effective use of this evaporative assembly approach. In this work, we therefore performed a synchrotron based X-ray photoemission study of BDMT evaporative adsorption onto Ag(111), Au(110), Cu(100), and Cu(111) surfaces, that allows us to shed light on a number of characteristics of the molecular layer formation.

2. EXPERIMENTAL METHOD

2.1. Photoemission. The measurements were carried out at the BEAR beamline (Elettra synchrotron radiation laboratory, Trieste, Italy). Photoemission spectra were acquired with a hemispherical deflection analyzer, with an overall energy resolution of <200 meV (analyzer and beamline, using a constant pass energy). Spectra were recorded at normal emission, with the light impinging at 45° with respect to the surface normal. We used $h\nu$ = 260 eV for Au 4f, S 2p, and Cu 3p levels, $h\nu$ = 380 eV for C 1s, $h\nu$ = 470 eV for Ag 3d, and $h\nu$ = 1050 eV for Cu 2p levels. These photon energies are in general chosen to maximize the surface sensitivity, measuring photoelectrons with kinetic energies corresponding to the minimum of the inelastic mean free path. The emission lines from Au 4f levels were acquired at each photon energy and were taken as an energy reference with Au $4f_{7/2}$ = 84.0 eV. We also measured the valence band at $h\nu$ = 60 eV. Since SAMs can be damaged by irradiation, we checked systematically for damage by measuring in several points on the sample and by comparing the spectra during a series of scans over the energy range under investigation.

2.2. Sample Preparation. Ag(111), Au(110), Cu(111), and Cu(100) single crystals were used as substrates. The samples were cleaned by sputtering and annealing cycles and their cleanliness ascertained by XPS and characteristics of valence band emission.

The samples were exposed to BDMT vapors, in the load lock of the preparation chamber. BDMT was placed in a vacuum sealed glass tube connected to the vacuum chamber through a valve. The tube containing the BDMT powder was kept at a constant temperature of about 80 °C, leading to BDMT melting. This allowed the vapor pressure to be increased during exposure. Several thaw−pump−"freeze" cycles were used to pump out before exposing the clean sample surface to the thiol vapors. The walls of the vacuum chamber used for exposure were preliminarily saturated with the organic molecules. The exposure is indicated in kilo or mega Langmuir (L, kL and ML). The samples were kept at room temperature during exposure. In some cases, we desorbed the BDMT layers by slow heating of the samples to a temperature of the order of 400 K for Cu and 450 K for Ag: a value estimated using a movable thermocouple which could be brought in contact with the sample holder.

3. RESULTS

In the following sections, we present our results on BDMT adsorption on Ag, Au, and Cu surfaces, starting with the Ag case. Some extra data is given in the Supporting Information in figures numbered S*n*.

3.1. SAMs of BDMT on Ag(111). *General Characteristics of BDMT Adsorption.* Recently, the evaporative adsorption of BDMT on Ag was studied by TOF-DRS[48] with Ar ion scattering and showed that at low exposures (a few thousand L) a lying down phase was formed, while a "standing up" BDMT layer with S "on top" was formed at large exposures. Here we investigated the characteristics of the BDMT layers formed under conditions of low and high exposures by photoemission. In adsorbing BDMT, we performed several sets of measurements in which the dosing procedure was varied to see in which manner this would affect the BDMT layer. As we shall see, some variability is observed and in the following we shall show S 2p XPS spectra that illustrate this.

Here we discuss results of the following exposure sequences:

(A) Following the work of Salazar Alarcón et al.,[48] the surface was first exposed to a small dose and thereafter to a large dose of BDMT. This should lead to an initial lying down phase and a subsequent standing up phase.[48]

(B) A direct large exposure, expected to lead to a standing up phase.

(C) A large exposure, performed in three successive dosing steps. A first high dose followed by two more dosings, after an interval of about 8 h (overnight).

In all these cases (A−C), the dosing was done rapidly over a period of a few minutes.

(D) A relatively large exposure over a longer, 1 h, exposure time.

The XPS spectra of the clean Ag(111) surface in the Ag 3d region and after BDMT exposure, following exposure sequence A, are shown in Figure 1a. The Ag binding energy is calibrated against Au $4f_{7/2}$ at 84.0 eV, and the Ag $3d_{5/2}$ peak position is found at 368.1 eV.

Upon exposure to 7 kL of BDMT vapors, the intensity of the Ag peak in Figure 1a decreases. The decrease of the Ag peak intensity is associated with the formation of a dithiol layer, leading to secondary electron scattering and attenuation of the signal. Further exposure to 0.9 ML leads to a larger decrease in Ag peak intensity signifying thickening of the layer.

An evaluation of the attenuation of the layers formed after the 7 kL and 0.9 ML exposures based on Ag 3d signal attenuation[24,27] and considering an inelastic mean free path Λ = 6 Å for the Au photoelectrons at 100 eV of kinetic energy in the

dx.doi.org/10.1021/jp509184t | J. Phys. Chem. C 2014, 118, 26866−26876

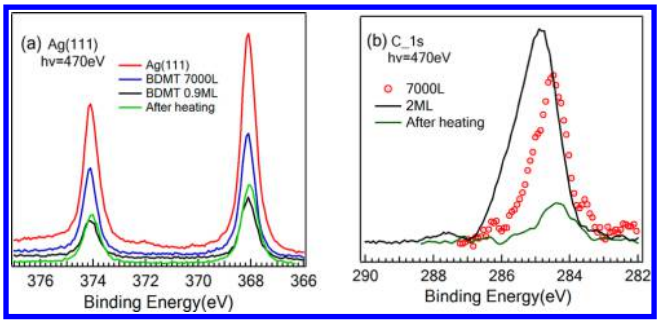

Figure 1. (a) XPS spectra of Ag 3d, showing intensity attenuation with different exposures and also after heating the exposed sample (see text). (b) XPS of C 1s for the indicated exposures and after heating.

organic film gives a BDMT effective thickness of 0.32 nm and about 0.7 nm, respectively. The thickness after the first exposure is compatible with lying down molecules, whereas at larger exposures the layer is thicker and is compatible with molecules that are in a "standing up" configuration. The latter thickness is close to but somewhat smaller than that for BDMT on Au(111), about 0.8−1 nm, determined using the same procedure.[24,27] Note that this thickness evaluation is not extended here to the case of the heated BDMT exposed Ag surface, since the nature of the surface layer is different, as will be discussed below.

The C 1s peak is shown in Figure 1b, for different situations: after the 7 kL exposure, after a large 2 ML exposure, and also after heating the sample to induce progressive BDMT desorption (see below). The initial C 1s spectrum peaks lie at about 284.4 eV in agreement with earlier studies and correspond to C atoms in the aromatic ring and in the methylene units, with contributions from a shake up satellite.[27] At high coverage, the peak shifts to higher binding energies of about 284.75 eV. This could be related to a reduced screening by the metal electrons of the core hole of carbon atoms when BDMT is in a standing up phase and to a weaker interaction of the molecule with the substrate. As will be discussed below, at very high coverages, there may be some physisorbed molecules on the SAM as well.

XPS S 2p spectra obtained in the various dosing procedures are shown in Figure 2.

Exposure A. After the first low (Figure 2a) exposure, we see that the spectrum is composed of a main doublet "T", at about 162 eV (in the following, we will refer to the peak position as the position of the S $2p_{3/2}$ component of the spin orbit split $2p_{3/2}-2p_{1/2}$ doublet), which is assigned to the thiolate S bonding to Ag. We also observe a smaller component ("A") at a lower binding energy. This spectrum is compatible with a lying down BDMT molecule configuration.

Deposition of more BDMT molecules (0.9 ML, Figure 2b) onto the lying down phase results in the appearance of an intense dominant peak around 163 eV. The 162 and 161 eV "T" and "A" peaks are also observed. The 163 eV peak (features F and P) can be assigned to unbound SH groups, on top of the SAM layer, as discussed below.

Exposure B. The result of a large dose of BDMT is shown in Figure 2c. The spectra were taken at normal and grazing emission. The spectrum taken at grazing emission angle shows that the 161 and 162 eV "T" and "A" components decrease in intensity with respect to the 163 eV "F" one, showing that the two former ones indeed correspond to S atoms not localized at the outer monolayer interface but below the organic layer. Feature "F" is assignable to S in the terminal groups of the

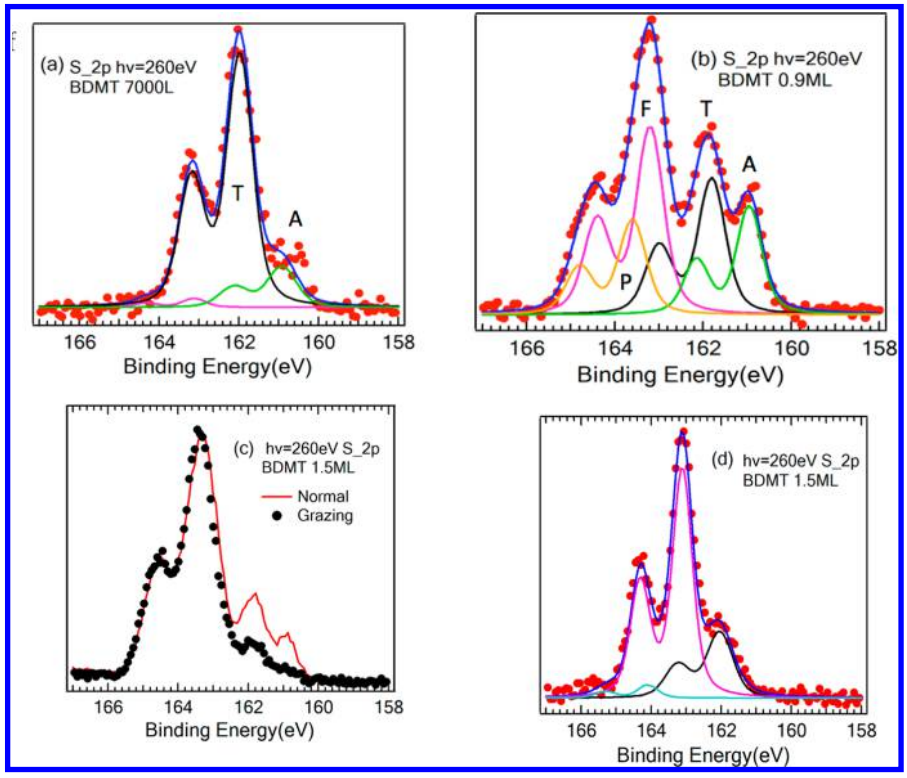

Figure 2. XPS spectra of the S 2p region for a 260 eV photon energy after a "small" (a) 7 kL exposure followed by a large (b) 0.9 ML exposure. (c) Spectra for normal (red line) and grazing (black points) angle emission for 1.5 ML exposure. The two spectra were normalized to the intensity of the most intense structure at 163 eV. (d) A different high 1.5 ML exposure spectrum (see text). Lines in panels a, b, and d correspond to fits (see text).

dx.doi.org/10.1021/jp509184t | J. Phys. Chem. C 2014, 118, 26866−26876

SAM's outer surface. We ascribe this to the formation of a standing up phase.

Exposure C. The exposure sequence C revealed some interesting features. Here the first exposure led to a spectrum similar to that in Figure 2b, with the extra "A" peak and had a maximum at 163.6 eV (see Figure S1a, Supporting Information). However, in the second exposure (Figure 2d), the "A" peak was not present, the main peak was at 163.1 eV, and the spectrum resembled the one observed in the case of a well ordered BDMT SAM, in liquid phase adsorption on Au(111).[27] The third exposure modified the BDMT layer again, and the spectrum changed to one with broader peaks, with again dominance of the 163.6 eV peak (Figure S1b, Supporting Information) and reappearance of peak "A". The "well ordered" spectrum in Figure 2d was not obtained in any other sets of measurements.

Exposure D. In this case, we exposed the surface to 340 kL over an hour, trying to dose slowly under conditions close to earlier works.[30,48] The result (Figure S2, Supporting Information) is similar to the spectra in Figure 2b and c.

We now examine the spectra in more detail. To fit the S 2p spectra of Figure 2a and b, we set the S $2p_{3/2-1/2}$ doublet components with a 1.2 eV spin orbit splitting and a branching ratio of 0.5 and the spectra are fitted using a Voigt contour after a Shirley background subtraction. A good fit of the spectrum in Figure 2b required four doublet components with S $2p_{3/2}$ at 160.95, 161.90, 163.15, and 163.60 eV given with an accuracy of 50 meV. We assign the 163.15 eV peak "F" to BDMT with free −SH.[24,27] The assignment of the 163.60 eV component "P" is more problematic. It could be assigned to formation of some disulfide bonds (−SS−), as discussed in some other studies.[37,50−53] Indeed, measurements on bulk-like films of dihexadecanedisulfide ($CH_3(CH_2)_{15}SS(CH_2)_{15}CH_3$) show that the binding energy for this case is about 163.5 eV.[52,53] There are however also reports[54] that for free alkanethiol molecules the binding energy for −SH is in the 163.5−164.0 eV range. Thus, it is quite plausible that, at very large exposures, some molecules stick to (or are physisorbed on) the SAM outer layer just as in an "unrinsed" SAM made in liquid.[54] We believe this is the more plausible assignment of this structure.

By analogy with the Au(111) case of some alkane and aromatic thiols[54−57] and dithiols,[22] we would assign the 160.95 eV component, "A" peak, to an alternative binding site on Ag. This assignment is supported by its transient appearance, as discussed in the exposure sequence C. This is similar to some earlier reports[55] for the case of thiol adsorption on Au, where a similar peak appeared only in initial phases of adsorption. Therefore, we do not favor the idea that it could be due to atomic sulfur resulting from, e.g., dissociation of BDMT with S−C bond scission.[59] Indeed, if bond cleavage would have occurred and was responsible for chemisorbed S atoms on the surface in the first exposure of the C sequence, then it should not disappear in the second exposure. We also do not believe that the 163 eV region peak here is related to beam damage, as shown by taking spectra at different points on the sample. The beam damage question is discussed in greater detail in the Supporting Information.

From the 0.7 nm thickness estimate, reported for dosing A above, which is less than what was measured for well ordered BDMT SAMs on Au[24,27] and the general form of the S 2p spectrum, we can conclude that we are not dealing with a good quality standing up SAM. This is visible in NEXAFS measurement (not shown here), where no clear changes were found between measurements for normal and grazing emission. This could be construed as due to (i) a large inclination of the molecules or due to poor order with (ii) some lying down phase still present and (iii) existence of physisorbed molecule on top of the SAM layer.

All the above experiments suggest that we do form a standing up dithiol layer, but frequently there are extra BDMT molecules sticking on top of the SAM leading to some type of multilayer formation. Furthermore, the frequent appearance of the "A" peak can be interpreted as being due to an alternative adsorption site that is not stable and is not observed in well ordered, standing up dithiol SAMs.

Some measurements were performed in the valence band region, and these results are given in the Supporting Information (Figure S3).

Ag Sulfidation. Previous TOF DRS measurements[48] show that, when the BDMT SAM is heated, changes appear above temperatures of about 100 °C and desorption occurs above 200 °C. Here we heated the sample to desorb the BDMT layer. In Figure 1b, we show the C 1s and in Figure 3 the S 2p regions

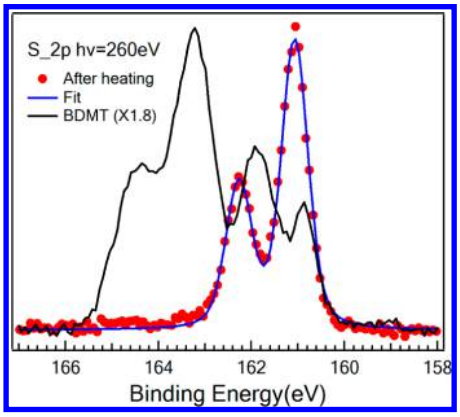

Figure 3. Comparison of the S 2p region before and after heating for the 0.9 ML exposure spectrum.

before and after annealing. One can see that after heating there is a strong attenuation of C 1s intensity, but the S 2p peak intensity remains quite high (Figure 3). Note that one could expect that the S 2p intensity from S remaining after BDMT dissociation and desorption will be higher, because the attenuation by the organic layer is no longer present. We can deduce that most of the thiolate S remains on the surface, whereas most of the carbon is removed. In these cases, the XPS spectra of the S 2p core level structure can be fitted with one doublet as shown.

In order to check if we deal simply with chemisorbed S or rather there is the possibility of Ag sulfidation, upon BDMT adsorption and after annealing, when mainly only S is present on the surface, we compare the line shapes of the Ag 3d peak (Figure 4a). We see that for BDMT adsorption the line shapes for the clean surface and for the surface with BDMT are similar (Figure 4a). However, the Ag(3d) peak after annealing is clearly slightly broader (Figure 4a,b), an effect we ascribe to sulfide formation.

To deduce the contribution from silver sulfide, first the Ag 3d peak of clean Ag is accurately fitted using a Voigt profile, shown in the inset of Figure 4b. The parameters of this fit are then used to define the shape of the Ag bulk peak (black, Ag_B), and we allow the other peak (violet) position to vary. We show the resulting spectral decomposition in Figure 4b. The peak

dx.doi.org/10.1021/jp509184t | J. Phys. Chem. C 2014, 118, 26866−26876

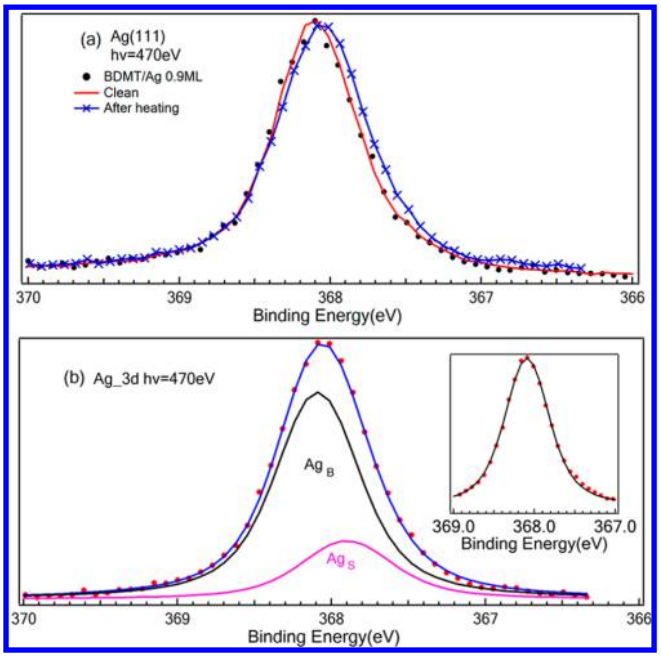

Figure 4. (a) Ag 3d peak shape for the clean surface, after 1 ML BDMT adsorption and after annealing. The spectral intensities were normalized for comparison. (b) Decomposition of the spectrum after annealing into a bulk Ag like (black) and the smaller (violet) sulfide Ag species (see text); the inset in part b shows the fit of the Ag $3d_{5/2}$ peak prior to BDMT adsorption.

position due to Ag sulfide (Ag_S) in this fit is found to be 367.9 eV. It is lower than that of the clean Ag peak (368.1 eV). This is similar to the case of selenization[59] and Ag oxidation[60] as well. Clearly for BDMT SAM adsorption, sulfidation does not occur, since the BDMT exposed and clean Ag peaks are essentially identical. Returning to the XPS spectra in Figure 3, we note that the sulfide S 2p peak appears to be at a slightly higher binding energy than the position of the peak assigned to the "alternative" adsorption site.

3.2. SAMs of BDMT on Au(110). Figure 5a shows the XPS spectrum in the Au($4f_{7/2}$) region for clean Au(110) and after exposure to BDMT, which leads to an attenuation of the peak intensity. From these measurements, one can estimate the thickness of the BDMT layer that is formed, using an attenuation length of 0.8 nm at a kinetic energy of 156 eV (for the 260 eV photon energy). The effective thickness of the BDMT layer was found to be 0.1 nm at 800 L, 0.56 nm at 12kL, and 1.56 nm at the highest exposure of 700 kL.

The thickness at low exposure is compatible with a lying down SAM, with possibly not a complete coverage. At intermediate exposures, we observe the formation of a standing up layer, which is thicker. The effective thickness is however less than that, observed for BDMT on Au(111) in liquid phase experiments.[24,27] At the highest exposure, the large thickness here suggests a multilayer formation (or that there is a large number of molecules physisorbed on top of the SAM).

Figure 5b shows the evolution of the C(1s) peak with exposure. One can note a steady increase in C intensity with increasing exposures. The peak position at intermediate exposures is at about 284.2 eV. This peak is associated with C atoms in the aromatic ring and in the methylene units, with contributions from a shake up satellite.[27] At low exposures, corresponding to mainly a lying down SAM, it is shifted toward lower energy. At the highest exposure, the peak moves to 284.5 eV. These changes are most probably due to changes in the interaction with the substrate, in particular to the progressively reduced screening of the metallic substrate on the C core holes at increasing coverage when the molecules adopt a standing orientation and when a multilayer is formed.

The evolution of the S 2p peak upon exposure to BDMT is shown in Figure 6. At the lowest exposure, we see mainly one doublet structure with the S($2p_{3/2}$) peak at about 161.8 eV corresponding to thiolate S. There is a small contribution at 163.1 eV due to unbound S, corresponding to some standing up BDMT molecules. With higher exposures, the intensity of the 163.1 eV peak increases, which may be attributed to an increase in standing BDMT. At the higher exposure of 12 kL, we also observe a shift of this peak toward 163.5 eV, as for the Ag case above. This is not due to X-ray damage in the film, as this was checked by measuring at different points on the sample as for Ag. At the highest exposure of 700 kL, there is a very strong change, with an almost complete disappearance of the 161.8 eV peak. This is attributed to formation of a multilayer (or to the fact that there is a large number of molecules physisorbed on top of the SAM). It is interesting that no extra peaks for S 2p, like the 161 eV "A" peak for Ag, appear here.

After heating the Au(110) sample, BDMT desorbed, as evidenced by the disappearance of the carbon peak, but some S remained on the surface (see Figure S5a, Supporting Information). The shape of the S 2p spectrum changed and there appeared a multicomponent structure, with an extra peak

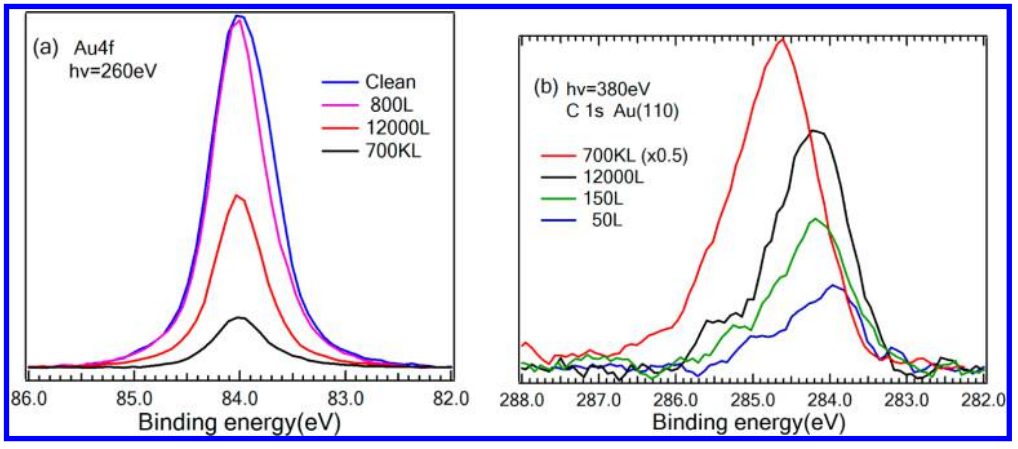

Figure 5. (a) XPS spectrum for Au $4f_{7/2}$ and (b) C 1s spectrum as a function of BDMT exposure.

dx.doi.org/10.1021/jp509184t | J. Phys. Chem. C 2014, 118, 26866−26876

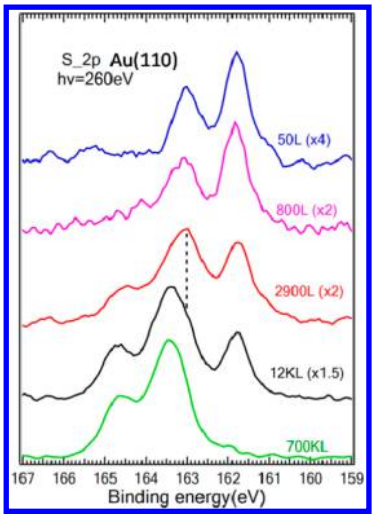

Figure 6. XPS spectrum in the S 2p region as a function of BDMT exposure.

close to 161 eV. A fit of the spectrum using Voigt doublets shows (Figure S5b, Supporting Information) that there are essentially two components at 161.2 and 161.9 eV. Clearly, this corresponds to two different adsorption configurations, with different S 2p core level binding energies.

3.3. SAMs of BDMT on Cu(100) and Cu(111). Recently, a study of BDMT adsorption on Cu(111) and Cu(100) surfaces was performed by time-of-flight direct recoil spectroscopy.[48,49] This study showed that in general adsorption proceeds "faster" than on Ag, i.e., lower exposures are necessary. As for the case of Ag(111), it showed that at high exposures a standing up layer of BDMT is formed, as deduced from the appearance of a peak due to recoiled (fast sputtered) S and a structure due to Ar scattering on the top S atoms. However, this study also revealed a rather intriguing feature: appearance of a S recoil peak in Kr bombardment, already at low exposures of the order of a few tens of Langmuir. A particularly curious aspect was that, after the initial, clear observation, the peak decreased in intensity and S was then observed more clearly at very high exposures. It is not obvious if what was observed was atomic S on the surface or there was some configuration of BDMT on the surface, for which in the initial phases of adsorption the SH group was "visible". Photoemission measurements are performed here to clarify this point.

Figure 7a shows the evolution of the Cu $2p_{3/2}$ peak intensity as a function of BDMT dosing on the Cu(100) surfaces. Figure 7b shows the evolution of the C(1s) peak. One can note a steady increase in C intensity with increasing exposures. The peak position at low to intermediate exposures is between 284.0 and 284.2 eV. As for the other cases discussed above, at low exposures corresponding to mainly a lying down SAM, it is shifted toward lower energy. At the highest exposure, the peak moves to 284.7 eV, because of decreasing interaction with the substrate, changes in screening effects, and some extra molecules sticking on top of the SAM. Results for Cu(111) were very similar and are not shown here (see Figure S6, Supporting Information).

The XPS spectra of the S 2p core level structure for different doses of BDMT adsorption on Cu(100) and Cu(111) are shown in Figure 8. At the highest exposures, we mainly see a doublet with a peak at 163.6 eV ascribable to a multilayer (Figure 8b).

At the low exposures for Cu(100), we see a main peak at about 161.4 eV and a secondary peak at about 162.3 eV (see fits in Figure 9). As the exposures increase, the intensity of the 162.3 eV peak grows and also that of the shoulder at about 163.5 eV, which then becomes prominent at high exposures. At the highest exposure of 700 kL, the 161 and 162 eV components are strongly attenuated. The spectrum is then like the one for the same exposure for Cu(111) shown in Figure 8b. For the case of Cu(111), measurements (Figure 8b) were only performed at 800 L, 12 kL, and 700 kL of exposure. In general, the spectra are very similar to the Cu(100) case.

For the Cu(100) case, we fitted the S 2p core level structure as shown in Figure 9. In the low exposure case, the spectra were fitted by two main doublets at 161.4 eV (marked "X") and 162.3 eV ("T") and one small doublet at higher energy at about 163.6 eV ("F"). At higher exposures, the "T" and "F" peak intensities increase relative to the "X" peak (see also Figure S7, Supporting Information).

In the existing literature,[33−44] it is known that, for alkane and benzene thiol on Cu, the core level binding energy of thiolate S bonded to Cu is around 162.4 eV. This is compatible with the second "T" doublet in Figure 9. What then is the origin of the "X", 161.4 eV, peak? As discussed for Au and Ag, one could consider that this may be an alternative adsorption site for BDMT on Cu. However, in the literature, one also finds several indications[33,34,38−40] that there may be spontaneous dissociation of thiols in some cases. This would seem to occur in the case of, e.g., alkanethiols[34,39] on Cu(100) and Cu(111) but not

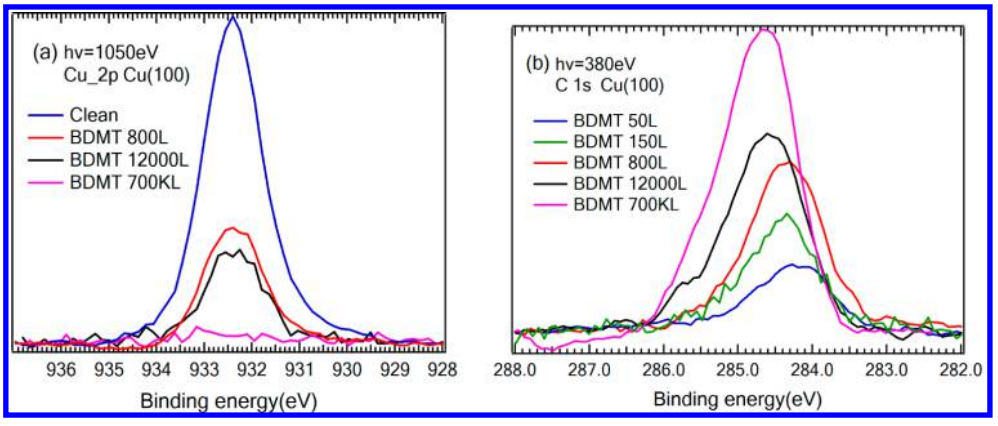

Figure 7. XPS spectrum in (a) the Cu $2p_{3/2}$ and (b) C 1s peak regions as a function of exposure to BDMT for Cu(100).

dx.doi.org/10.1021/jp509184t | J. Phys. Chem. C 2014, 118, 26866−26876

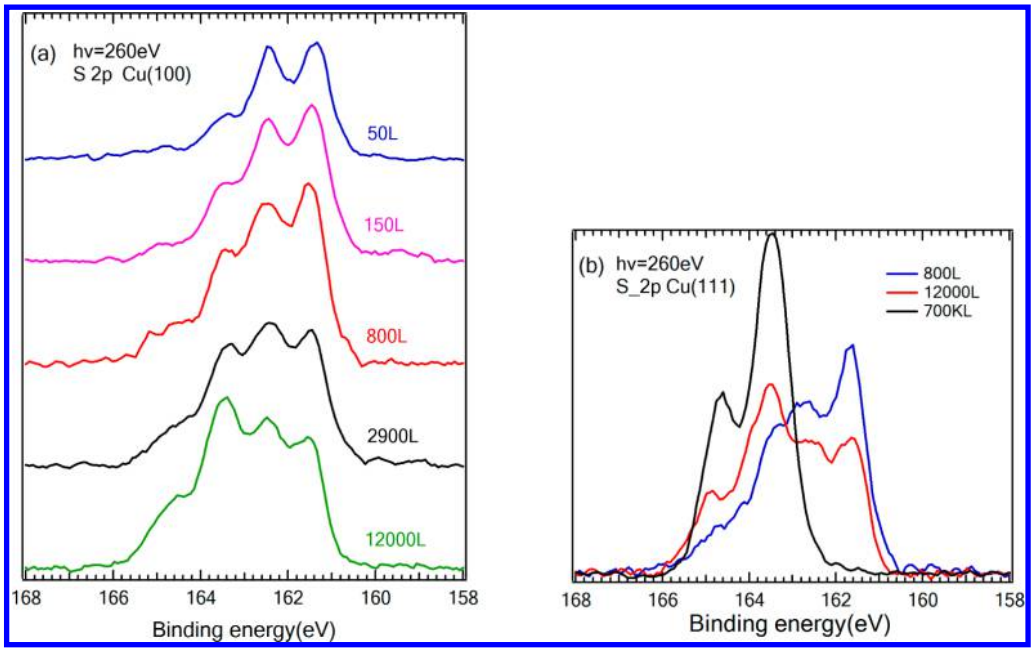

Figure 8. S 2p peak XPS spectra for (a) Cu(100) and (b) Cu(111) for the indicated exposures.

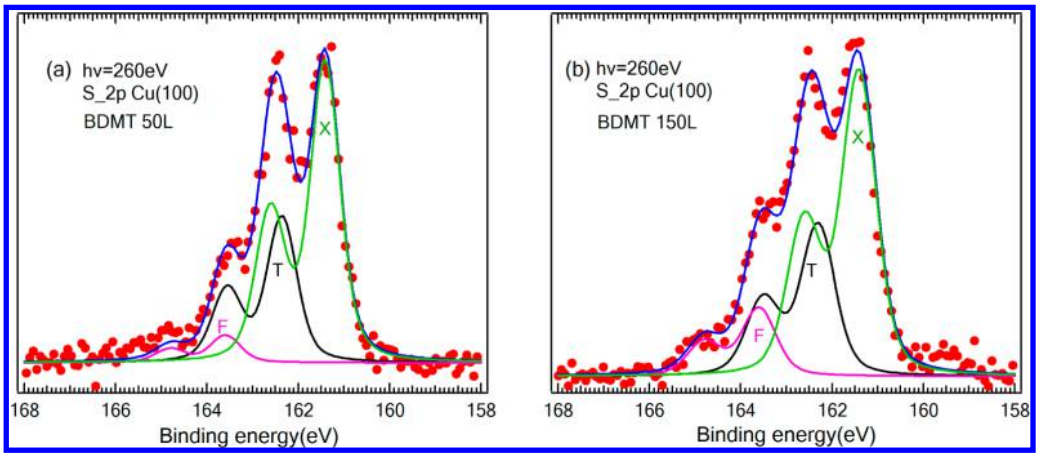

Figure 9. XPS spectra for BDMT adsorption on the Cu(100) surface: (a) 50 L; (b) 150 L.

for benzenethiol on Cu(100).[41] The TOF-DRS data mentioned above showed also appearance of an S recoil at very low exposures.

To answer this question, plots of the intensity evolution of S 2p, C 1s, and Cu 2p peaks as a function of dose are shown in Figure 10. The intensity for each measurement is normalized to the photon flux determined for the BEAR beamline. We see a decrease in Cu 2p intensity and at the same time an increase in C 1s and also S 2p intensity. One notices immediately that the C 1s intensity (hollow squares) is low with respect to the S 2p one (red circles). In principle, for a lying down BDMT molecule, one can expect that, at the lowest coverage, we should see the intensity of the S 2p peak 4 times smaller than the C 1s intensity because BDMT molecules consist of eight C atoms, while the number of S atoms is two. Since there are differences in the photionization cross sections for C 1s and S 2p at the photon energies used here (380 and 260 eV), we corrected for this by multiplying the C 1s peak intensity by a factor of 4.89, which takes these differences into account. The C 1s intensity is then still only slightly higher than that of S 2p, as shown in Figure 10 (black filled squares).

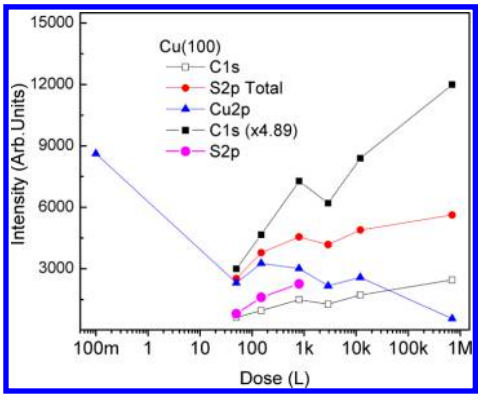

Figure 10. Intensity evolution of S 2p, C 1s, and Cu 2p peaks as a function of dose. The black squares correspond to the C 1s intensity corrected for differences in the photoionization cross section. The indigo circles correspond to the intensity of the S 2p peak without the contribution of the 161 eV doublet (see text).

To understand the reason behind this discrepancy, we re-evaluate the S 2p intensity using the fitted spectra in Figure 9,

dx.doi.org/10.1021/jp509184t | J. Phys. Chem. C 2014, 118, 26866−26876

after subtracting out the "X", 161.4 eV, peak, as shown with the pink points in Figure 10. We now get almost 4 times less S 2p than C 1s intensity. This clearly suggests that the 162.3 eV peak is due to thiolate S of the BDMT molecules, while 161.4 eV must be an extra S atomic peak due to BDMT dissociation. Note that the Cu(100) sample has been used in a number of other studies and does not show any signs of S segregation after high temperature annealing. We therefore rule out any S segregation effects.

It is difficult to conduct this procedure for the higher exposures, as clearly the BDMT molecules are "standing up" and then one needs to incorporate appropriate attenuation factors for electrons passing through the BDMT layer. This is not included in the 800 L data in Figure 10, though such a correction would need to be included. Indeed, as one can see in Figure 9a, the contribution of the 163.6 eV peak starts to increase, although it is still small, so the correction would be small.

On the basis of our data, it is plausible that for the Cu(111) case this dissociation is also occurring. Indeed, the S 2p spectra are similar to the Cu(100) case, as may be seen in, e.g., the 800 L case in Figure 10. For the 800 L exposure, an evaluation of the S to C ratio, after inclusion of corrections for photon flux and photoionization cross sections, shows that there is nearly the same amount of sulfur and carbon, showing thus excess sulfur. The existence of atomic sulfur thus results in the appearance of the 161.4 eV peak, like for Cu(100).

We conclude that in BDMT adsorption spontaneous S−C bond cleavage occurs on both Cu(100) and Cu(111). This happens in the initial stages of adsorption. Subsequently, BDMT adsorption occurs on the S containing Cu surface. Presumably, this happens after initial passivation of the surface reactivity.

This behavior can explain the initial appearance and intermediate attenuation of the S peak in TOF-DRS measurements mentioned above. In these measurements, one first observes S from dissociation, which is then screened by the adsorbed BDMT. Later one observes the S from the standing up BDMT. Adsorption of the molecule after initial scission of the S−C bonds implies of course that the remaining cleaved molecule leaves the surface. Possibly this could happen with the cleaved end passivated by the extra hydrogen:

$$HS{-}CH_2{-}C_6H_4{-}CH_2{-}SH + Cu \rightarrow SCu + HS{-}CH_2{-}C_6H_4{-}CH_3$$

A theoretical investigation of such a reaction pathway would be interesting.

We also investigated the effect of heating on these BDMT exposed samples. After heating the sample (Figure 11), we observed only traces of remaining C and the S 2p peak underwent a strong change, consisting of one doublet at about 161.4 eV. This binding energy is compatible with known binding energies[41,61] for Cu(100) sulfidation, and for known ordered[62] phases of S on Cu surfaces. For S on Cu(111)[63] for the latter cases, the CLBEs have been found to be 161.45 and 161.15 eV depending on coverage, whereas for Cu(100)[63] for higher coverages of the order of 0.47 monolayers they are equal to 161.15, 161.62, and 162.10 eV and for lower coverages 161.05 and 164.45 eV. BDMT desorption thus left S adsorbed on the surface. The energy resolution at the rather high Cu 2p energy was insufficient here to make any definite conclusions about copper sulfide formation.

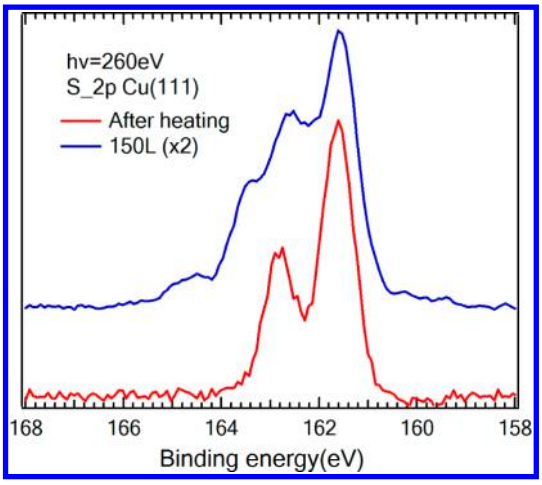

Figure 11. S 2p spectra for BDMT on Cu(100) before and after annealing.

The evolution of the spectra in the valence band region was investigated and is given in the Supporting Information, with some comments based on earlier work.[64]

4. SUMMARY AND CONCLUSIONS

The experiments on BDMT adsorption from the vapor phase on Au(110) and Ag(111) reveal that at low exposures a lying down BDMT phase with both S atoms attached to Ag is formed. A standing up phase could be attained after a large exposure above several tens of thousand Langmuir. This follows from thickness estimates and because in the standing up phase the S $2p_{3/2}$ core level structure at about 163 eV is dominant in the XPS spectra. However, we usually observe both a 163.1 eV peak due to the BDMT−SH[27] and also a 163.6 eV peak, which could be assigned to both −SH[54] and −SS[53,57,58] groups. Also, for Ag(111), we observe a peak close to the 161 eV, which we attribute to an alternative binding site of BDMT molecules. NEXAFS measurements did not indicate the unambiguous presence of a standing up ordered SAM. From these results, one can conclude that, while we do form a standing up dithiol SAM, at high exposures there are extra BDMT molecules sticking on top of the SAM, thus leading to a thicker layer formation and some molecules are adsorbed on alternative adsorption sites.

After heating the sample, BDMT desorbs, leaving some S atoms following S−C bond scission. In the case of Au, some S atoms are left in different adsorption sites with mainly two different core level binding energies. In the case of Ag, sulfidation occurs, as concluded from the Ag(3d) peak shape changes, and our analysis shows that the Ag sulfide component is at a lower binding energy, as for oxidation and selenization of Ag. In this case, the S 2p peak can be fitted with only one doublet.

In the case of Cu(100) and Cu(111) at fairly high exposures, one observes appearance of "standing up" molecules. At the highest exposures, some multilayer formation is also observed. Here we also observe an "extra" S $2p_{3/2}$ component at 161.45 eV. The main difference from the case of Au and Ag is that, in this case of a more reactive surface, our analysis shows that adsorption is accompanied by some degree of S−C bond cleavage. Some BDMT molecules lose S, which is adsorbed on Cu. The 161.45 eV peak can thus be related to S atoms from dissociation. This dissociation would seem to occur in the initial

dx.doi.org/10.1021/jp509184t | J. Phys. Chem. C 2014, 118, 26866−26876

phases of dosing. Thereafter, surface passivation occurs. The dissociation process then slows down and BDMT adsorption then occurs on a Cu surface with S present from dissociation. In this context, it should be pointed out that formation of thiol SAMs on a sulfidized interface layer has been earlier reported for a Pd surface,[65,66] in a similar process of initial dissociation and passivation of the surface. Further investigation of the structure of this CuS interface would be most welcome. Finally, it is also interesting to point out that this spontaneous dissociation has not been observed for benzenethiol adsorption on these surfaces.[41]

■ ASSOCIATED CONTENT

Supporting Information

S 2p XPS spectra for Ag, Au, and Cu with BDMT for different exposures and after annealing. X-ray damage for BDMT on Ag. Valence band spectrum for Ag(111) and Cu(100) with BDMT. This material is available free of charge via the Internet at http://pubs.acs.org.

■ AUTHOR INFORMATION

Corresponding Author

*E-mail: vladimir.esaulov@u-psud.fr. Phone: +33169157680.

Notes

The authors declare no competing financial interest.

■ ACKNOWLEDGMENTS

J.J. thanks the Chinese Scholarship Council for her Ph.D. scholarship. This work was performed partly in the framework of the France-Chile ECOS Sud program (No. C12E02) and is supported also by CNRS French-Argentina International Laboratory for Nanoscience (LIFAN). M.F. thanks the Fondecyt project 1140759.

■ REFERENCES

(1) Andres, R. P.; Bein, T.; Dorogi, M.; Feng, S.; Henderson, J. I.; Kubiak, C. P.; Mahoney, W.; Osifchin, G. R.; Reifenberger, R. Coulomb Staircase at Room Temperature in a Self-Assembled Molecular Nanostructure. *Science* **1996**, *272*, 1323−1325.

(2) Andres, R. P.; Bielefeld, J. D.; Henderson, J. I.; Janes, D. B.; Kolagunta, V. R.; Kubiak, C. P.; Mahoney, W. J.; Osifchin, R. G. Self-Assembly of a Two-Dimensional Superlattice of Molecularly Linked Metal Clusters. *Science* **1996**, *273*, 1690−1693.

(3) Loo, Y.-L.; Lang, D. V.; Rogers, J. A.; Hsu, J. W. P. Electrical Contacts to Molecular Layers by Nanotransfer Printing. *Nano Lett.* **2003**, *3*, 913−917.

(4) Akkerman, H. B.; Naber, R. C. G.; Jongbloed, B.; Van Hal, P. A.; Blom, P. W. M.; de Leeuw, D. M.; de Boer, B. Electron Tunneling Through Alkanedithiol Self-Assembled Monolayers in Large-Area Molecular Junctions. *Proc. Natl. Acad. Sci. U.S.A.* **2007**, *104*, 11161−11166.

(5) Kobayashi, K.; Horiuchi, T.; Yamada, H.; Matsushige, K. STM Studies on Nanoscopic Structures and Electric Characteristics of Alkanethiol and Alkanedithiol Self-Assembled Monolayers. *Thin Solid Films* **1998**, *331*, 210−215.

(6) Aliganga, A. K. A.; Lieberwirth, I.; Glasser, G.; Duwez, A.-S.; Sun, Y.; Mittler, S. Fabrication of Equally Oriented Pancake Shaped Gold Nanoparticles by SAM-Templated OMCVD and Their Optical Response. *Org. Electron.* **2007**, *8*, 161−174.

(7) Loo, Y.-L.; Lang, D. V.; Rogers, J. A.; Hsu, J. W. P. Electrical Contacts to Molecular Layers by Nanotransfer Printing. *Nano Lett.* **2003**, *3*, 913−917.

(8) Hsu, J. W. P.; Lang, D. V.; West, K. W.; Loo, Y.-L.; Halls, M. D.; Raghavachari, K. Probing Occupied States of the Molecular Layer in Au−Alkanedithiol−GaAs Diodes. *J. Phys. Chem. B* **2005**, *109*, 5719−5723.

(9) Hamoudi, H. Bottom-Up Nanoarchitectonics of Two-Dimensional Freestanding Metal Doped Carbon Nanosheet. *RSC Adv.* **2014**, *4*, 22035−22041.

(10) Hamoudi, H.; Uosaki, K.; Ariga, K.; Esaulov, V. A. Going Beyond The Self-Assembled Monolayer: Metal Intercalated Dithiol Multilayers and Their Conductance. *RSC Adv.* **2014**, *4*, 39657−39666.

(11) Krapchetov, D. A.; Ma, H.; Jen, A. K. Y.; Fischer, D. A.; Loo, Y.-L. Deprotecting Thioacetyl-Terminated Terphenyldithiol for Assembly on Gallium Arsenide. *Langmuir* **2008**, *24*, 851−856.

(12) Rifai, S.; Morin, M. Isomeric Effect on the Oxidative Formation of Bilayers of Benzenedimethanethiol on Au(111). *J. Electroanal. Chem.* **2003**, *550−551*, 277−289.

(13) Rieley, H.; Kendall, G. K.; Zemicael, F. W.; Smith, T. L.; Yang, S. X-ray Studies of Self-Assembled Monolayers on Coinage Metals. 1. Alignment and Photooxidation in 1,8-Octanedithiol and 1-Octanethiol on Au. *Langmuir* **1998**, *14*, 5147−5153.

(14) Liang, J.; Rosa, L. G.; Scoles, G. Nanostructuring, Imaging and Molecular Manipulation of Dithiol Monolayers on Au(111) Surfaces by Atomic Force Microscopy. *J. Phys. Chem. C* **2007**, *111*, 17275−17284.

(15) Pugmire, D. L.; Tarlov, M. J.; Van Zee, R. D. Structure of 1,4-Benzenedimethanethiol Self-Assembled Monolayers on Gold Grown by Solution and Vapor Techniques. *Langmuir* **2003**, *19*, 3720−3726.

(16) Joo, S.-W.; Han, S. W.; Kim, K. Adsorption Characteristics of p-Xylene-α,α'-dithiol on Gold and Silver Surfaces: Surface-Enhanced Raman Scattering and Ellipsometry Study. *J. Phys. Chem. B* **1999**, *103*, 10831−10837.

(17) Carot, M. L.; Esplandiu, M. J.; Cometto, F. P.; Patrito, E. M.; Macagno, V. A. Reactivity of 1,8-Octanedithiol Monolayers on Au(111): Experimental and Theoretical Investigation. *J. Electroanal. Chem.* **2005**, *579*, 13−23.

(18) Hamoudi, H.; Dablemont, C.; Esaulov, V. A. Disorder, Solvent Effects and Substitutional Self-Assembly of Alkane Dithiols From Alkane Thiol SAMs. *Surf. Sci.* **2011**, *605*, 116−120.

(19) Leung, T. Y. B.; Gerstenberg, M. C.; Lavrich, D. J.; Scoles, G.; Schreiber, F.; Poirier, G. E. 1,6-Hexanedithiol Monolayers on Au(111): A Multitechnique Structural Study. *Langmuir* **2000**, *16*, 549−561.

(20) Zareie, H. M.; McDonagh, A. M.; Edgar, J.; Ford, M. J.; Cortie, M. B.; Phillips, M. R. Controlled Assembly of 1,4-Phenylenedimethanethiol Molecular Nanostructures. *Chem. Mater.* **2006**, *18*, 2376−2380.

(21) García-Raya, D.; Madueño, R.; Blázquez, M.; Pineda, T. Formation of 1,8-Octanedithiol Mono- and Bilayers under Electrochemical Control. *J. Phys. Chem. C* **2010**, *114*, 3568−3574.

(22) Jia, J.; Mukherjee, S.; Hamoudi, H.; Nannarone, S.; Pasquali, L.; Esaulov, V. A. Lying-Down to Standing-Up Transitions in Self Assembly of Butanedithiol Monolayers on Gold and Substitutional Assembly by Octanethiols. *J. Phys. Chem. C* **2013**, *117*, 4625−4631.

(23) Chaudhari, V.; Harish, M. N. K.; Srinivasan, S.; Esaulov, V. A. Substitutional Self-Assembly of Alkanethiol and Selenol SAMs from a Lying-Down Doubly Tethered Butanedithiol SAM on Gold. *J. Phys. Chem. C* **2011**, *115*, 16518−1652.

(24) Hamoudi, H.; Prato, M.; Dablemont, C.; Cavalleri, O.; Canepa, M.; Esaulov, V. A. Self-Assembly of 1,4-Benzenedimethanethiol Self-Assembled Monolayers on Gold. *Langmuir* **2010**, *26*, 7242−7247.

(25) Hamoudi, H.; Guo, Z. A.; Prato, M.; Dablemont, C.; Zheng, W. Q.; Bourguignon, B.; Canepa, M.; Esaulov, V. A. On the Self-Assembly of Short Chain Alkanedithiols. *Phys. Chem. Chem. Phys.* **2008**, *10*, 6836−6841.

(26) Daza Milone, M. A.; Hamoudi, H.; Rodríguez, L. M.; Rubert, A.; Benitez, G. A.; Vela, M. E.; Salvarezza, R. C.; Gayone, J. E.; Sánchez, E. A.; et al. Self-Assembly of Alkanedithiols on Au(111) from Solution: Effect of Chain Length and Self-Assembly Conditions. *Langmuir* **2009**, *25*, 12945−12953.

(27) Pasquali, L.; Terzi, F.; Seeber, R.; Nannarone, S.; Datta, D.; Dablemont, C.; Hamoudi, H.; Canepa, M.; Esaulov, V. A. A UPS, XPS

and NEXAFS Study of Self-Assembly of Standing 1,4-Benzenedimethanethiol SAMs on Gold. *Langmuir* **2011**, *27*, 4713−4720.
(28) Pasquali, L.; Terzi, F.; Zanardi, C.; Pigani, L.; Seeber, R.; Paolicelli, G.; Suturin, S. M.; Mahne, N.; Nannarone, S. Structure and Properties of 1,4-Benzenedimethanethiol Films Grown from Solution on Au(111): An XPS and NEXAFS Study. *Surf. Sci.* **2007**, *601*, 1419−1427.
(29) Pasquali, L.; Terzi, F.; Seeber, R.; Doyle, B. P.; Nannarone, S. Adsorption Geometry Variation of 1,4-Benzenedimethanethiol Self-Assembled Monolayers on Au(111) Grown from the Vapor Phase. *J. Chem. Phys.* **2008**, *128*, 134711.
(30) Salazar Alarcón, L.; Chen, L.; Esaulov, V. A.; Gayone, J. E.; Sánchez, E. A.; Grizzi, O. Thiol Terminated 1,4-Benzenedimethanethiol Self-Assembled Monolayers on Au(111) and InP(110) from Vapor Phase. *J. Phys. Chem. C* **2010**, *114*, 19993−19999.
(31) Pasquali, L.; Mukherjee, S.; Terzi, F.; Giglia, A.; Mahne, N.; Koshmak, K.; Esaulov, V.; Toccafondi, C.; Canepa, M.; Nannarone, S. Structural and Electronic Properties of Anisotropic Ultrathin Organic Films from Dichroic Resonant Soft X-ray Reflectivity. *Phys. Rev. B* **2014**, *89*, 045401.
(32) Rodríguez, L. M.; Gayone, J. E.; Sánchez, E. A.; Ascolani, H.; Grizzi, O.; Sánchez, M.; Blum, B.; Benitez, G.; Salvarezza, R. C. Adsorption of Short-Chain Alkanethiols on Ag(111) Studied by Direct Recoiling Spectroscopy. *Surf. Sci.* **2006**, *600*, 2305−2316.
(33) Shen, W.; Nyberg, G. L.; Liesegang, J. An Electron Spectroscopic Study of the Adsorption of and 1,2-Benzenedithiol on the Cu(110) Surface. *Surf. Sci.* **1993**, *298*, 143−160.
(34) Vollmer, S.; Witte, G.; Wöll, C. Structural Analysis of Saturated Alkanethiolate Monolayers on Cu(100): Coexistence of Thiolate and Sulfide Species. *Langmuir* **2001**, *17*, 7560−7565.
(35) Beccari, M.; Pomponio, S.; Castro, V. D. Self-Assembly of Para-Substituted Benzenethiols on Copper: an XPS Study. *Superlattices Microstruct.* **2009**, *46*, 25−29.
(36) Caprioli, F.; Beccari, M.; Martinelli, A.; Castro, V. D.; Decker, F. A Multi-Technique Approach to the Analysis of SAMs of Aromatic Thiols on Copper. *Phys. Chem. Chem. Phys.* **2009**, *11*, 11624−11630.
(37) Laiho, T.; Leiro, J. A.; Heinonen, M. H.; Mattila, S. S.; Lukkaric, J. Photoelectron Spectroscopy Study of Irradiation Damage and Metal−Sulfur Bonds of Thiol on Silver and Copper Surfaces. *J. Electron Spectrosc. Relat. Phenom.* **2005**, *142*, 105−112.
(38) Wada, S.; Takigawa, M.; Matsushita, K.; Kizaki, H.; Tanaka, K. Adsorption and Structure of Methyl Mercaptoacetate on Cu(1 1 1) Surface by XPS and NEXAFS Spectroscopy. *Surf. Sci.* **2007**, *601*, 3833−3837.
(39) Syed, J. A.; Sardar, S. A.; Yagi, S.; Tanaka, K. Orientation of Ethanethiol on Cu(111): Low and Room Temperature Adsorption. *Thin Solid Films* **2006**, *515*, 2130−2136.
(40) Lai, Y.-H.; Yeh, C.-T.; Liao, P.; Hung, W.-H. Adsorption and Thermal Decomposition of Alkanethiols on Cu(110). *J. Phys. Chem. B* **2002**, *106*, 5438−5446.
(41) Beccaria, M.; Kanjilal, A.; Betti, M. G.; Mariani, C.; Floreano, L.; Cossaro, A.; Castro, V. D. Characterization of Benzenethiolate Self-Assembled Monolayer on Cu(100) by XPS and NEXAFS. *J. Electron Spectrosc. Relat. Phenom.* **2009**, *172*, 64−68.
(42) Furlong, O. J.; Miller, B. P.; Li, Z.; Walker, J.; Burkholder, L.; Tysoe, W. T. The Surface Chemistry of Dimethyl Disulfide on Copper. *Langmuir* **2010**, *26*, 16375−16380.
(43) Allegretti, F.; Bussolotti, F.; Woodruff, D. P.; Dhanak, V. R.; Beccari, M.; Mariani, C. The Local Adsorption Geometry of Benzenethiolate on Cu(100). *Surf. Sci.* **2008**, *602*, 2453−2462.
(44) Kin, L.; Wong, K.-Y. K.; Bartels, L. Surface Dynamics of Benzenethiol Molecules on Cu(111). *Appl. Phys. Lett.* **2006**, *88*, 183106.
(45) Lim, J. K.; Kwon, O.; Joo, S.-W. Interfacial Structure of 1,3-Benzenedithiol and 1,3-Benzenedimethanethiol on Silver Surfaces: Surface-Enhanced Raman Scattering Study and Theoretical Calculations. *J. Phys. Chem. C* **2008**, *112*, 6816−6821.
(46) Denayer, J.; Delhalle, J.; Mekhalif, Z. Self-Assembly of Amine Terminated Alkylthiol and Alkyldithiol Films on a Polycrystalline Copper Substrate. *J. Electrochem. Soc.* **2011**, *158*, 100−108.
(47) Esaulov, V. A. Low Energy Ion Scattering and Recoiling Spectroscopy in Surface Science. In *Surface Science Techniques*; Bracco, G., Holst, B., Eds.; Springer Series in Surface Science; Springer: Berlin, 2013; Vol. *51*, pp 423−460.
(48) Salazar Alarcón, L.; Cristina, L. J.; Shen, J.; Jia, J.; Esaulov, V. A.; Sánchez, E. A.; Grizzi, O. Growth of 1,4-Benzenedimethanethiol Films on Au, Ag, and Cu: Effect of Surface Temperature on the Adsorption Kinetics and on the Single Versus Multilayer Formation. *J. Phys. Chem. C* **2013**, *117*, 17521−17530.
(49) Salazar Alarcón, L.; Jia, J.; Carrera, A.; Esaulov, V. A.; Ascolani, H.; Gayone, J. E.; Sánchez, E. A.; Grizzi, O. Direct Recoil Spectroscopy of Adsorbed Atoms and Self-Assembled Monolayers on Cu(001). *Vacuum* **2014**, *105*, 80−87.
(50) Shaporenko, A.; Terfort, A.; Grunze, M.; Zharnikov, M. A. A Detailed Analysis of the Photoemission Spectra of Basic Thioaromatic Monolayers on Noble Metal Substrates. *J. Electron Spectrosc. Relat. Phenom.* **2006**, *151*, 45−61.
(51) Zerulla, D.; Chasse, T. X-ray Induced Damage of Self-Assembled Alkanethiols on Gold and Indium Phosphide. *Langmuir* **1999**, *15*, 5285−5294.
(52) Heister, K.; Zharnikov, M.; Grunze, M.; Johansson, L. S. O.; Ulman, A. Characterization of X-ray Induced Damage in Alkanethiolate Monolayers by High-Resolution Photoelectron Spectroscopy. *Langmuir* **2001**, *17*, 8−11.
(53) Hamoudi, H.; Chesneau, F.; Patze, C.; Zharnikov, M. Chain-Length-Dependent Branching of Irradiation-Induced Processes in Alkanethiolate Self-Assembled Monolayers. *J. Phys. Chem. C* **2011**, *115*, 534−541.
(54) Castner, D. G.; Hinds, K.; Grainger, D. W. X-ray Photoelectron Spectroscopy Sulfur 2p Study of Organic Thiol and Disulfide Binding Interactions with Gold Surfaces. *Langmuir* **1996**, *12*, 5083−5086.
(55) Ishida, T.; Hara, M.; Kojima, I.; Tsuneda, S.; Nishida, N.; Sasabe, H.; Knoll, W. High Resolution X-ray Photoelectron Spectroscopy Measurements of Octadecanethiol Self-Assembled Monolayers on Au(111). *Langmuir* **1998**, *14*, 2092−2096.
(56) Ito, E.; Kang, H.; Lee, D.; Park, J. B.; Hara, M.; Noh, J. Spontaneous Desorption and Phase Transitions of Self-Assembled Alkanethiol and Alicyclic Thiol Monolayers Chemisorbed on Au(1 1 1) in Ultrahigh Vacuum at Room Temperature. *J. Colloid Interface Sci.* **2013**, *394*, 522−529.
(57) Frey, S.; Stadler, V.; Heister, K.; Eck, W.; Zharnikov, M.; Grunze, M.; Zeysing, B.; Terfort, A. Structure of Thioaromatic Self-Assembled Monolayers on Gold and Silver. *Langmuir* **2001**, *17*, 2408−2415.
(58) Gonella, G.; Cavalleri, O.; Terreni, S.; Cvetko, D.; Floreano, L.; Morgante, A.; Canepa, M.; Rolandi, R. High Resolution X-Ray Photoelectron Spectroscopy of 3-Mercaptopropionic Acid Self-Assembled Films. *Surf. Sci.* **2004**, *566−568*, 638−643.
(59) Jia, J.; Bendounan, A.; Kotresh, H. M. N.; Chaouchi, K.; Sirotti, F.; Sampath, S.; Esaulov, V. A. Selenium Adsorption on Au(111) and Ag(111) Surfaces: Adsorbed Selenium and Selenide Films. *J. Phys. Chem. C* **2013**, *117*, 9835−9842.
(60) Gronbeck, H.; Klacar, S.; Martin, N. M.; Hellman, A.; Lundgren, E.; Andersen, J. N. Mechanism for Reversed Photoemission Core-Level Shifts of Oxidized Ag. *Phys. Rev. B* **2012**, *85*, 115445.
(61) Kundu, M.; Hasegawa, T.; Terabe, K.; Yamamoto, K.; Aono, M. Structural Studies of Copper Sulfide Films: Effect of Ambient Atmosphere. *Sci. Technol. Adv. Mater.* **2008**, *9*, 035011.
(62) Colaianni, M. L.; Chorkendorff, I. Scanning-Tunneling-Microscopy Studies of the S- Induced Reconstructions of Cu(100). *Phys. Rev. B* **1994**, *50*, 8798−8806.
(63) Jia, J.; Bendounan, A.; Chaouchi, K.; Esaulov, V. A. Sulfur Interaction with Cu(100) and Cu(111) Surfaces: a Photoemission Study. *J. Phys. Chem. C* **2014**, *118*, 24583−24590.
(64) Ling, D. T.; Miller, J. N.; Weissman, D. L.; Pianeta, P.; Stefan, P. M.; Lindau, I.; Spicer, W. E. An Angle-Resolved Photoemission Study

of the Chemisorption of Chalcogens on Cu(100) III. Cu(100) + p(2 × 2)S. *Surf. Sci.* **1983**, *124*, 175−187.
(65) Love, J. C.; Wolfe, D. B.; Haasch, R.; Chabinyc, M. L.; Paul, K. E.; Whitesides, G. M.; Nuzzo, R. G. Formation and Structure of Self-Assembled Monolayers of Alkanethiolates on Palladium. *J. Am. Chem. Soc.* **2003**, *125*, 2597−2609.
(66) Jia, J.; Bendounan, A.; Chaouchi, K.; Kubsky, S.; Sirotti, F.; Pasquali, L.; Esaulov, V. A. Chalcogen Atom Interaction with Palladium and the Complex Molecule-Metal Interface in Thiol Self Assembly. *J. Phys. Chem. C* **2014**, DOI: 10.1021/jp507051q.